

Surface-induced fragmentation of higher fullerenes and endohedral metallofullerenes

Takumi Kimura, Toshiki Sugai, and Hisanori Shinohara^{a)}

Department of Chemistry, Nagoya University, Nagoya 464-8602, Japan

(Received 21 December 1998; accepted 19 February 1999)

We report the first results of surface collisions of pure hollow fullerenes (C_{60} , C_{70} and C_{78}) and endohedral metallofullerenes ($Y@C_{82}$, $Ca@C_{82}$ and $Ca@C_{84}$), isolated by liquid chromatography, against solid (silicon and gold) surfaces and self-assembled monolayer (SAM) films. The experiments have been performed by a reflectron type time-of-flight mass spectrometer modified for measuring surface-induced dissociation (SID) spectra. No surface-induced fragment is observed for the surface collisions with the solid surfaces and the alkanethiolate SAM film. In contrast, sequential C_2 -loss fragments have been observed for the surface collisions of hollow fullerenes and $Ca@C_{84}$ with the fluorinated SAM film. © 1999 American Institute of Physics. [S0021-9606(99)01219-2]

I. INTRODUCTION

Surface-induced fragmentation studies of fullerenes¹⁻³ with various solid surfaces have played an important role in characterizing their structures and reactivity. The molecular dynamics (MD) simulations⁴ on collisions of C_{60} with a hydrogen-terminated diamond surface have shown a very strong deformation of C_{60} with no fragmentation at collision energy of 250 eV because of its structural resilience against a surface impact. Whetten and co-workers¹ reported the absence of surface-induced fragments of C_{60} even at collision energies up to 200 eV against a silicon and a highly oriented pyrolytic graphite (HOPG) surface. They found that the collision processes were highly inelastic and the scattered C_{60} lost a major part of its initial kinetic energy on collision. In contrast, Hertel and co-workers² reported that surface-induced fragments of C_{60} colliding with an HOPG surface were seen at collision energies above 275 eV.

Surface-induced dissociation (SID) phenomena strongly depend on not only the structure of an incident ion but also the surface composition. Kappes and co-workers³ reported that a translational-to-internal energy transfer of collided C_{60}^+ ions on an HOPG covered by hydrocarbon adsorbates differs significantly from that on an HOPG surface cleaned by heating at 1000 °C. In this context, SAM (self-assembled monolayer) films are shown to be useful surfaces for SID experiments, which were introduced and developed by Cooks and co-workers on surface impact studies.⁵ The SAM films are prepared in solution by spontaneous assembly of 1-alkanethiols (or their derivatives) onto a gold or a silver surface, which form highly ordered and covalently bonded monolayer films. They are stable under ambient and vacuum condition and have little surface contamination, which can easily be removed by the solvent washing. Cooks and co-workers⁵ have performed a series of SID experiments of polyatomic ions on SAM films with various terminal functional groups on the alkane chains. They found that a fluori-

nated SAM film provides the most effective translational-to-internal energy conversion compared to the other alkanethiolate surfaces. A part of the translational energy (12%) was converted into the internal energy on the alkanethiolate surface collisions, whereas the fluorinated surface was a more effective target, showing a 19% translational-to-internal energy conversion under typical impact conditions.⁵

Neutralization efficiency upon surface impact is also an important factor to observe and characterize the scattered ions in the SID experiment. The total scattered ion abundance, which is a good indicator of the neutralization probability, was found to vary as a function of the chain length of the alkanethiolate.⁶ Chemical composition of SAM films also affects the neutralization efficiency and a fluorinated SAM film gives the highest total scattered ion signal.⁶ The fluorinated SAM film is an effective surface also for the SID study of fullerenes. Callahan *et al.*⁷ studied the collisions of C_{60}^+ and C_{60}^{2+} with the fluorinated and the alkanethiolate SAM films. They found that the fluorinated surface causes greater conversion of the kinetic energy into the internal energy: more extensive fragmentation of C_{60}^{2+} was observed in collisions with the fluorinated surface than in collisions with the alkanethiolate surface.

In the present study, we have investigated collisions of fullerenes and metallofullerenes with solid (silicon and gold) surfaces and self-assembled monolayer (SAM) films with a fluorinated and an alkanethiolate surface. We have found that the collision processes such as a translational-to-internal energy transfer and a charge transfer between the collided ion and the surface strongly depend on the composition of surfaces.

II. EXPERIMENT

Figure 1 shows a schematic diagram of a reflectron type time-of-flight (TOF) mass spectrometer modified for measuring SID spectra. The details of the apparatus have been de-

^{a)} Author to whom correspondence should be addressed.

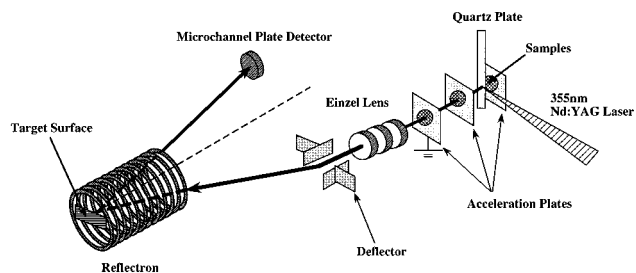


FIG. 1. A schematic diagram of a reflectron type time-of-flight mass spectrometer modified for measuring SID (surface-induced dissociation) spectra.

scribed previously.⁸ The experimental set-up is similar to that of Whetten and co-workers¹ and Brenner and co-workers.⁹

A quartz plate, which was drop-coated by a carbon disulfide extract of fullerenes or metallofullerenes, was mounted in an ion acceleration region of the TOF mass spectrometer. The desorption/ionization was done by the third harmonic of a Nd:YAG laser (Spectra Physics GCR 150) at 355 nm. The pulsed acceleration voltage was typically in the range of 1500–2000 V with 10 μ s duration. The accelerated ions were focused by an einzel lens into the ion reflector and then collided with a target surface mounted at the bottom of the ion reflector. The target surface can be heated up to 400 °C by a contacted heater to remove surface impurities while monitoring the temperature with a thermocouple.

The collision energy, $E_{\text{collision}}$, is given by the difference between the kinetic energy, U_0 , of the incident ions and the static electric potential energy, U_s , which is applied to the surface,

$$E_{\text{collision}} = U_0 - U_s.$$

The scattered ions were accelerated by the same electric field of the ion reflector and detected by a chevron-type dual microchannel plates (Galileo Electro-Optics 93M0028). The time-of-flight ion signals were accumulated over 200–500 shots and were analyzed on a transient digitizer (LeCroy 9400A). The conversion from time to mass scale and the analysis of the obtained TOF and SID spectra were performed on a personal computer (NEC PC9801-RA).

A schematic representation of (a) an alkanethiolate and (b) a fluorinated SAM film is shown in Fig. 2. The details of the preparation of the SAM films have been described

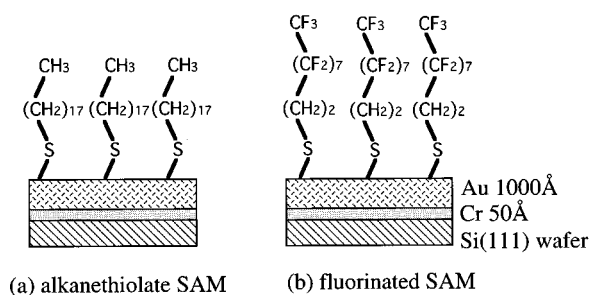


FIG. 2. A schematic representation of (a) an alkanethiolate and (b) a fluorinated SAM film.

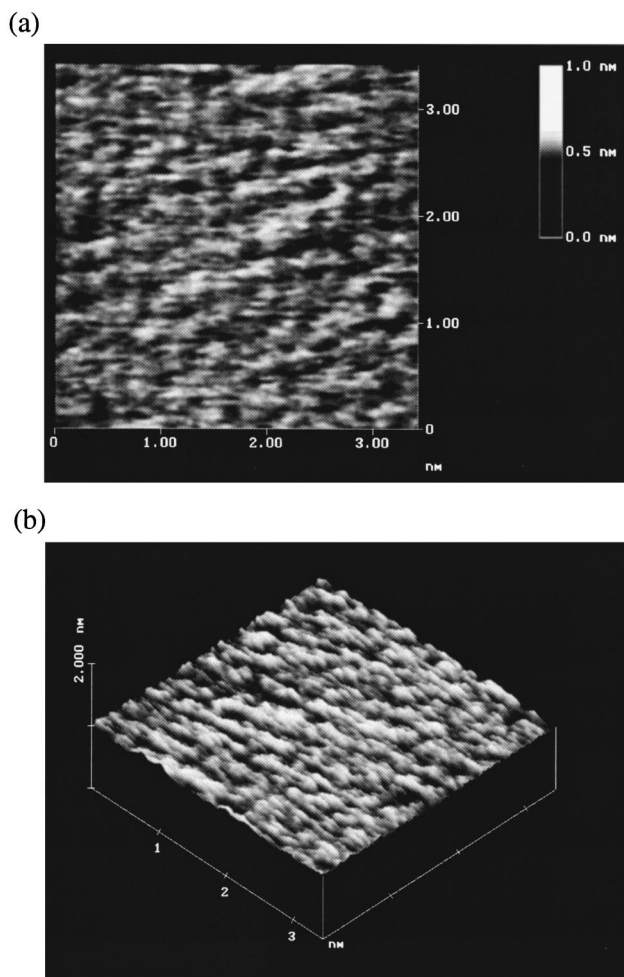


FIG. 3. AFM images of (a) a top view and (b) a side view of a fluorinated SAM film.

elsewhere.^{5–8} Briefly, a gold film (1000 Å) was vapor-deposited on a silicon (111) wafer with a chromium under-layer (50 Å). The gold film was cleaned by oxygen plasma for 15 min. and rinsed in methanol several times, and was then immersed for approximately 2 days in 1 mM solution of octadecanethiolate [$\text{CH}_3(\text{CH}_2)_{17}\text{SH}$] and 2-(perfluorooctyl)-ethanethiol [$\text{CF}_3(\text{CF}_2)_7\text{CH}_2\text{CH}_2\text{SH}$] to prepare the alkanethiolate and the fluorinated SAM films, respectively. 2-(perfluorooctyl)-ethanethiol was synthesized from the corresponding iodide [$\text{CF}_3(\text{CF}_2)_7\text{CH}_2\text{CH}_2\text{I}$] by a standard procedure.¹⁰

Atomic force microscopy (AFM) images of a fluorinated SAM film, which was prepared on a cleaved mica by the same procedure described above, is shown in Fig. 3. The AFM observation was performed at room temperature by a Nanoscope III AFM (Digital Instruments Inc.). The observed nearest-neighbor distance between the fluorinated chains is 4.4 Å, which is in qualitative agreement with the reported value (5.7 Å).¹¹

Fullerenes (C_{60} , C_{70} and C_{78}) and metallofullerenes (Y@C_{82} , Ca@C_{82} and Ca@C_{84}) were produced by a direct-current (300–500 A) contact arc-discharged method under a He flow at 50 Torr. The details of the apparatus with an anaerobic soot sampling mechanism for fullerenes produc-

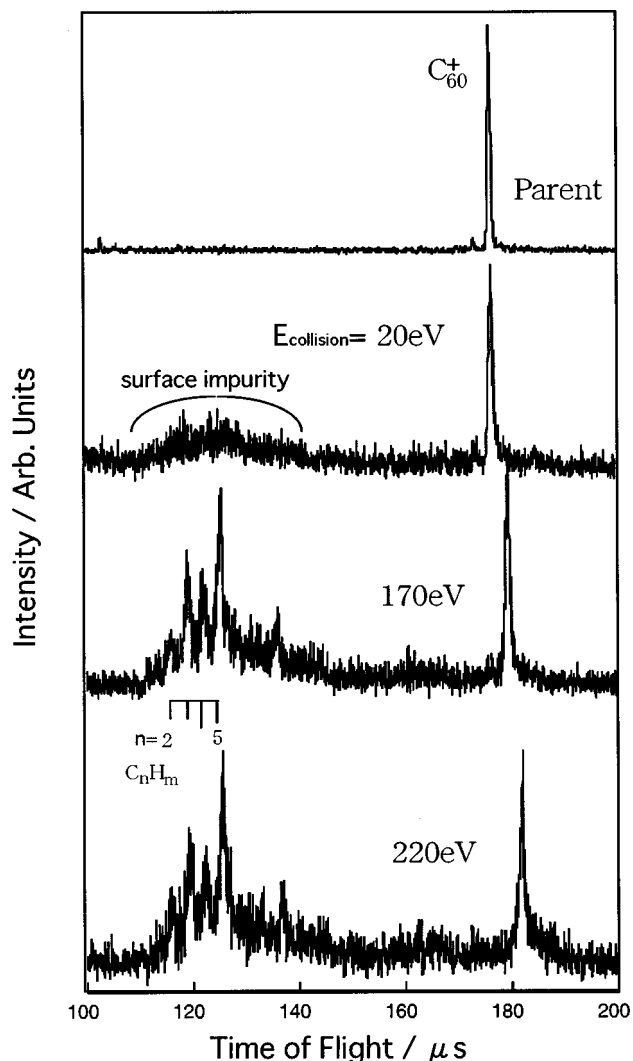


FIG. 4. Surface-induced dissociation spectrum of C_{60}^+ against a Si (111) surface over collision energies ranging from 20 to 220 eV.

tion have been described previously.^{12–15} The carbon soot so produced was collected under totally anaerobic conditions to avoid unnecessary contamination from the air and was Soxhlet extracted by carbon disulfide or, in some cases, refluxed with pyridine. The fullerenes or metallofullerenes were separated and isolated by the so-called two-stage high performance liquid chromatography (HPLC; Japan Analytical Industry LC-908-C60) method.^{14–17}

III. RESULTS AND DISCUSSION

A. Fullerene impacts against silicon surface

Figure 4 shows SID spectra for collisions of C_{60}^+ with a Si (111) surface over a range from 20 to 220 eV. No surface-induced fragment is seen even at collision energies up to 220 eV. The results are remarkably similar to that obtained for the surface collision of C_{60}^+ with a Si (100) surface by Whetten and co-workers.¹ As a reference, we have performed a SID experiment of anthracene ($C_{14}H_{10}^+$) on the same experimental set-up. The results showed extensive surface-induced fragments $C_nH_m^+$ ($n = 2–13$) upon collision (120 eV

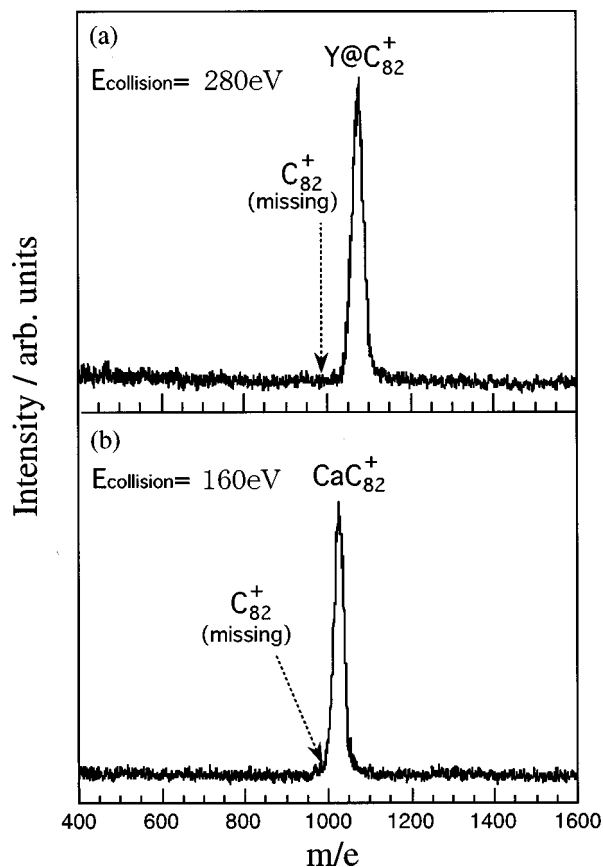


FIG. 5. Surface-induced dissociation spectra of (a) $Y@C_{82}^+$ and (b) $Ca@C_{82}^+$ against a Si (111) surface at collision energies of 280 and 160 eV, respectively.

collision energy) with the Si(111) surface (not shown). This indicates unusual stability of C_{60} against surface impact as reported earlier.¹

Signals appearing in the low mass region correspond to small hydrocarbons (C_nH_m ; $n = 2–5$) which increase as the collision energy increases. This is due to sputtering of the surface impurities by C_{60}^+ , since the hydrocarbons decreased on a similar collision with the silicon surface heated at 400 °C. In addition, we have found that the total intensity of the scattered C_{60}^+ ions also decreased when the surface was heat treated. This is because of the fact that a charge transfer is effectively occurring between the collided C_{60}^+ and the cleaned silicon surface.

SID spectra of HPLC-purified $Y@C_{82}^+$ and $Ca@C_{82}^+$ with the silicon surface (not heated) are shown, respectively, in Figs. 5(a) and 5(b). In Fig. 5(a), since C_{82}^+ produced from the intact $Y@C_{82}^+$ ion is not seen, no direct yttrium-stripping fragmentation is occurring up to the collision energy 280 eV. This is consistent with the fact that the Y atom is engaged by the C_{82} fullerene as proved by a synchrotron x-ray diffraction result.¹⁸ Similarly, no direct calcium-stripping fragmentation for $Ca@C_{82}^+$ is observed up to 160 eV collision energies [Fig. 5(b)]. This strongly supports that $Ca@C_{82}$ also has an endohedral structure. If $Ca@C_{82}$ has an exohedral structure, $Ca(C_{82})$, the Ca atom should be dissociated from the C_{82} cage upon collision processes. In fact, externally bound metallofullerenes such as $Fe(C_{60})^+$ (Ref. 19) and $La(C_{60})^+$ (Ref.

20), which are produced by the reaction between laser-vaporized metal ions and thermally vaporized C_{60} , have been known to eject the metal atoms on collisions with Ar atoms even at low impact energies (~ 5 eV in center-of-mass energies). Whetten and co-workers²¹ performed a similar SID experiment and concluded that $La_2@C_{80}$ has an endohedral structure. They also found no lanthanum-stripping fragmentation of $La_2@C_{80}^-$ against a Si(100) surface even at collision energies up to 190 eV.

B. Collisions against gold surface

To investigate the influence of surface composition, we performed SID experiments of $Ca@C_{82}$ on a gold surface. In the case of $Ca@C_{82}^+$, the SID feature (i.e., no surface-induced fragmentation) is similar to that observed in the collision with the silicon surface. Lill *et al.*²² reported that C_{60}^+ collisions with transition metal surfaces such as Ni(100) and Cu(100) did not show any detectable scattered ions because of the strong interaction between π -electrons of the C_{60}^+ cage and the transition metal surfaces. However, the scattering intensity of $Ca@C_{82}^+$ was similar to that observed for the silicon surface, indicating that virtually no surface reaction was occurring on the (inert) gold surface upon surface impact.

We have also performed a SID experiment of the $Ca@C_{82}^-$ anion. SID spectra for collisions of $Ca@C_{82}^-$ with a gold surface are shown in Fig. 6. Signals due to collision-induced detached electrons are seen. It is known that an electron emission efficiency of carbon cluster anions upon collision with a solid surface strongly depends on their structures (linear-chains, rings and fullerenes).²³ As seen in Fig. 6, again no surface-induced fragmentation was found at energies of up to 270 eV (3.3 eV/atom). The result is consistent with a reported molecular dynamics (MD) calculation for C_{60} impact on an Au(111) surface, which showed that fragmentation takes place at kinetic energies above 4 eV/atom.²⁴ Kappes and co-workers²⁵ have reported that the collision of $La@C_{82}^+$ on an HOPG surface showed C_2 -loss fragments above 120 eV collision energies. The results indicate that a translational-to-internal energy transfer efficiency of the gold surface is lower than that of the HOPG surface. This is partly because of the softness of the gold crystal with a weak metallic binding as compared with the fullerene carbon cage, and the collision mainly causes the damage to the surface in the current collision energies.

C. Collisions against self-assembled monolayer (SAM) films

As seen so far, no surface-induced fragment of fullerenes or metallofullerenes was observed on the silicon and the gold surfaces. This is not only due to a remarkable resilience of the fullerene molecules but also due to softness of the oxygen-passivated silicon surface as well as the gold surface, which causes a low translational-to-internal energy transfer of collided ions. Figure 7 shows SID spectra for collisions of C_{60}^+ with a fluorinated SAM film over a wide energy range from 50 to 200 eV. In contrast to the silicon and the gold surfaces, extensive surface-induced fragments

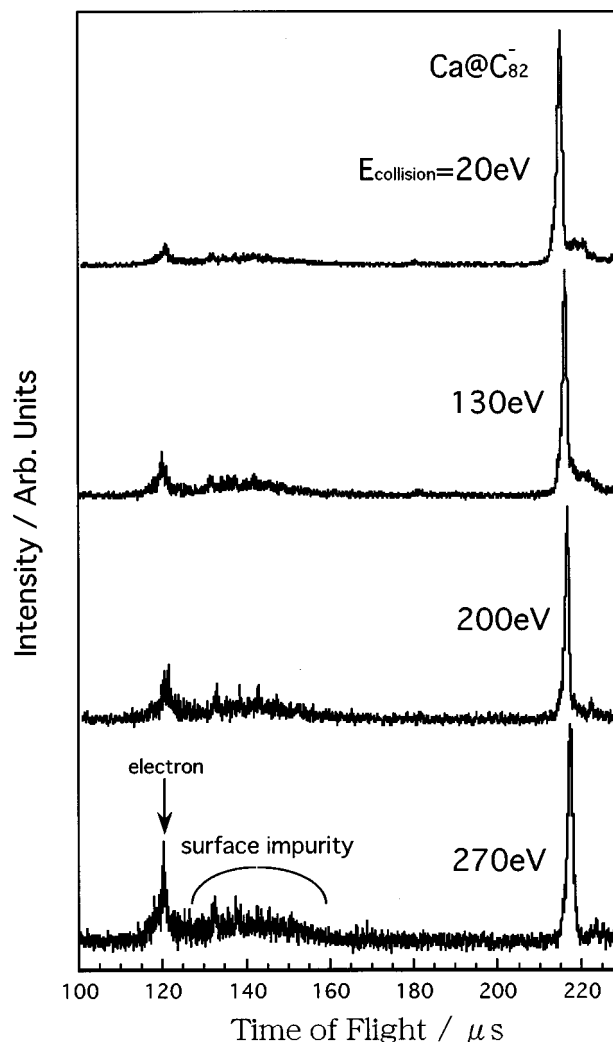


FIG. 6. Surface-induced dissociation spectrum of $Ca@C_{82}^-$ against a gold surface over collision energies ranging from 20 to 270 eV.

such as C_{58}^+ and C_{56}^+ , resulting from sequential C_2 -loss processes, are seen above 90 eV collision energies. This result is similar to that reported by Callahan *et al.*⁷ Figure 8 shows SID spectra for collisions of C_{70}^+ with the fluorinated SAM film over a range from 130 to 230 eV. The fragment distribution of C_{70}^+ is qualitatively similar to that of C_{60}^+ . The distribution consists of a series of even numbered fragments (C_{2n}^+) with an enhanced peak at C_{60}^+ due to a particularly stable structure, suggesting that surface-induced fragments have fullerene structures. Similar C_2 -loss fragment features were also observed for C_{78}^+ (not shown).

Figure 9(a) shows a TOF mass spectrum of the parent $Ca@C_{84}^+$ before the surface impact, indicating the high purity of the $Ca@C_{84}^+$ sample. Figure 9(b) shows a SID spectrum (220 eV collision energy) of $Ca@C_{84}^+$ with the fluorinated SAM film. In contrast to Fig. 5(b), C_2 -loss SID fragments such as CaC_{82}^+ and CaC_{80}^+ are seen in Fig. 9(b). The C_2 -loss feature is similar to those observed in the fragmentation of hollow fullerenes (C_{60} , C_{70} and C_{78}). In the present study, however, it is not clear whether or not direct calcium-strip-

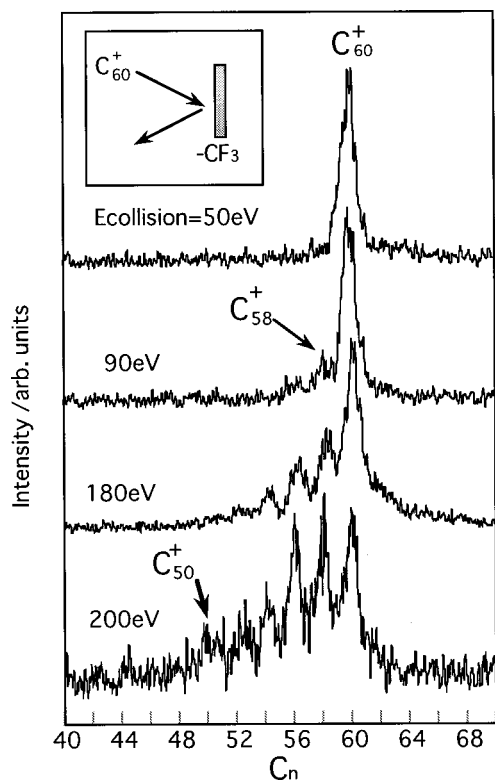


FIG. 7. Surface-induced dissociation spectrum of C_{60}^+ against a fluorinated SAM film over collision energies ranging from 50 to 200 eV.

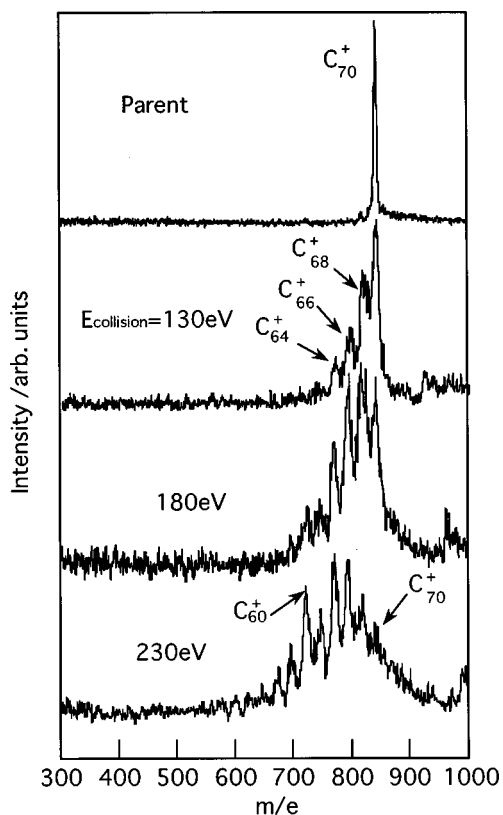


FIG. 8. Surface-induced dissociation spectrum of C_{70}^+ against a fluorinated SAM film over collision energies ranging from 130 to 230 eV.

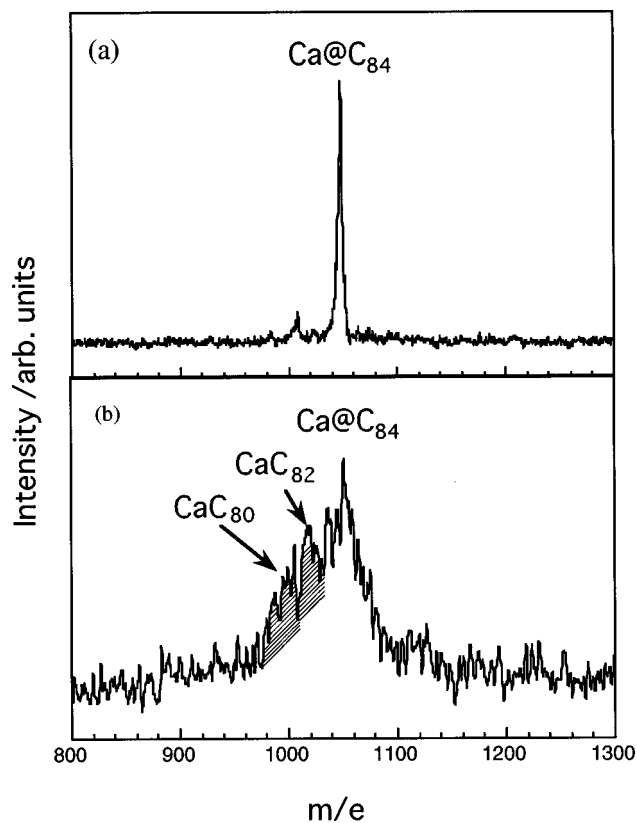


FIG. 9. (a) Laser-desorption/ionization TOF mass spectrum of parent $Ca@C_{84}^+$ before surface impact. (b) Surface-induced dissociation spectrum of $Ca@C_{84}^+$ against a fluorinated SAM film at a collision energy of 220 eV.

ping fragmentation is occurring due to the insufficient mass resolution.

The internal energy (E_i) of a scattered C_{60}^+ ion on the fluorinated surface is given by

$$E_i = E_{\text{collision}} - E_k - Q_{\text{surface}},$$

where E_k is a kinetic energy of scattered C_{60}^+ and Q_{surface} is an absorbed energy for the surface at collision. In Fig. 10, the flight times of scattered intact C_{60}^+ ions are plotted against collision energies, along with simulated curves which are obtained by assuming an inelastic ($e=0$ and 0.5) and a totally elastic ($e=1$) scattering process. The elastic coefficient, e , is defined as the ratio of the recoil velocity to the incident velocity. The observed TOF of the scattered intact C_{60}^+ is in good agreement with that calculated assuming a totally inelastic collision process ($e=0$). The TOF analysis indicates that the scattered C_{60}^+ lost a major part of its perpendicular momentum of the initial kinetic energy upon collision, which was also observed in the collision processes of fullerenes¹ and hexafluorobenzene (C_6F_6)_n⁻ clusters²⁶ on an HOPG and a silicon surface, respectively. A large part of collision energy ($E_{\text{collision}}$) is converted to the internal energy of the scattered ion (E_i) and to heat the surface (Q_{surface}).

Cooks and co-workers⁵ estimated that a translational-to-internal energy transfer was 19% and the energy taken up by the surface was 60% for the collisions of $W(CO)_6^+$ with a fluorinated SAM surface. Based on this, it is expected that the scattered C_{60}^+ has enough internal energy to exceed the

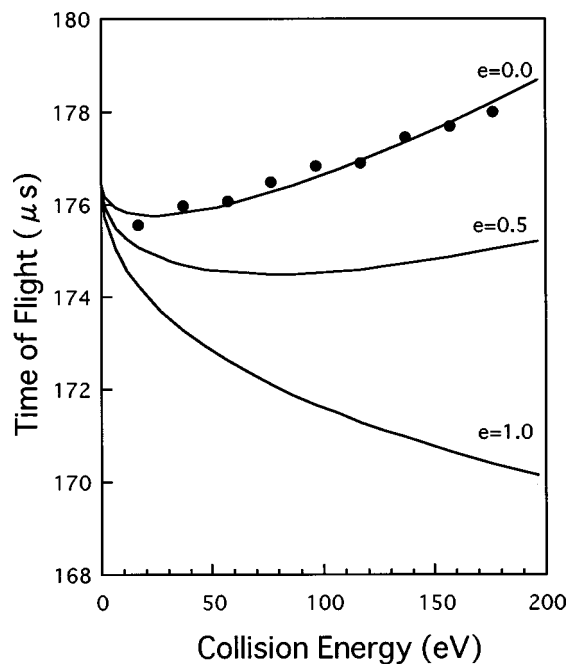


FIG. 10. The flight time of the scattered intact C_{60}^+ against collision energies, along with simulated curves which are obtained by assuming inelastic ($e=0$ and $e=0.5$) and a totally inelastic ($e=1$) scattering processes.

C_2 -loss barrier (10–14 eV)^{2,27} even at the present 90 eV collision energy, although its initial internal energy by laser desorption is not previously known. The energy transfer ratio of the fluorinated SAM surface (19%)⁵ is somewhat higher than that of an HOPG surface (15%) as suggested by a Rice–Ramsperger–Kassel–Marcus (RRKM)-calculation.³ In fact,

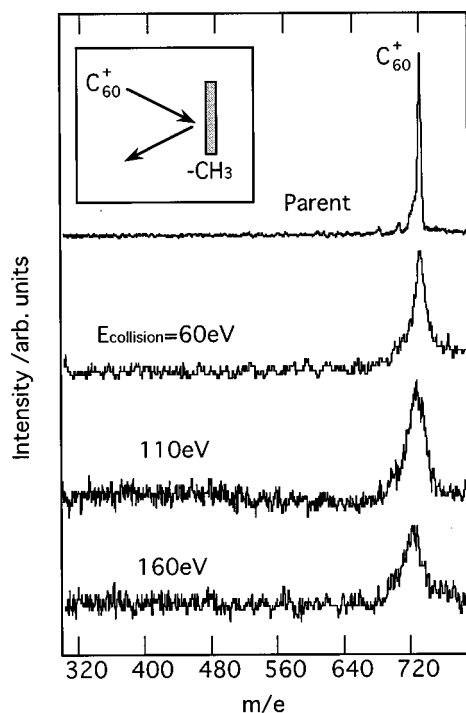


FIG. 11. Surface-induced dissociation spectrum of C_{60}^+ against an alkanethiolate SAM film over collision energies ranging from 60 to 160 eV.

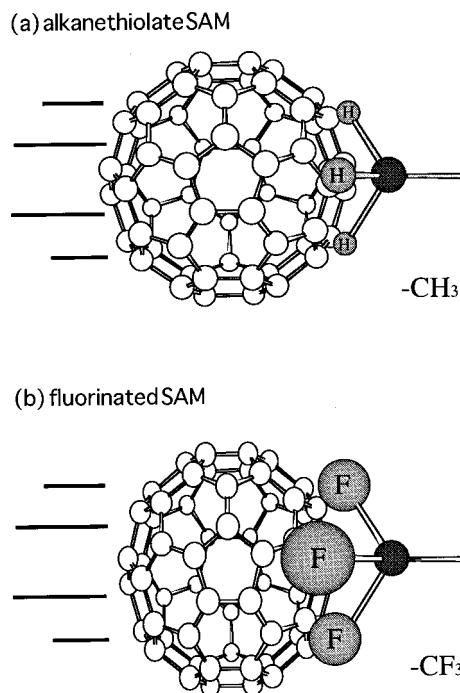


FIG. 12. Illustration of the collision processes of C_{60}^+ against (a) an alkanethiolate and (b) a fluorinated SAM film.

we can observe C_2 -loss fragments at lower collision energies than those observed in HOPG surfaces.^{2,3}

Figure 11 shows SID spectra of C_{60}^+ against an alkanethiolate SAM film over collision energies from 60 to 160 eV. Above 160 eV, enough signals for mass analysis were not possible to detect because of the meager intensities. The total yield of the scattered C_{60}^+ against the alkanethiolate SAM film was 1/4 of that against the fluorinated SAM film at a 160 eV collision energy: neutralization efficiency is much higher upon the collision with the alkanethiolate SAM film than with the fluorinated film. A higher ionization energy of the fluorinated SAM film (e.g., $IE[C_3F_8]=13.4$ eV) than that of the alkanethiolate (e.g., $IE[C_{10}H_{22}]=9.65$ eV) reduces the charge transfer between C_{60}^+ and the surface.

In contrast to the fluorinated SAM film, no SID of C_{60}^+ is observed for an alkanethiolate SAM film (Fig. 11). Obviously, the alkanethiolate SAM film generates less effective translational-to-internal energy transfer of the collided C_{60}^+ ions than the fluorinated SAM film. The difference in the transfer efficiency of an incident kinetic to an internal energy can be explained by an impulsive model for a surface collision of a polyatomic ion.²⁸ The model predicts that the energy transfer efficiency from a kinetic to an internal energy increases as an effective surface mass increases, which is determined by the mass of the functional group hit by the incident ion. Illustrations of the collision processes of C_{60}^+ against the alkanethiolate and the fluorinated SAM films are shown in Figs. 12(a) and 12(b), respectively. In the present case, F atoms of the fluorinated SAM film are larger in mass than H atoms of the alkanethiolate SAM film, which causes a greater momentum transfer at the collision event.

IV. SUMMARY

Virtually no surface-induced fragment of fullerenes or metallofullerenes was observed with the silicon and the gold surfaces. This is not only due to a remarkable resilience of the fullerene molecule but also due to softness of the oxygen-passivated silicon and the gold surface, which causes low translational-to-internal energy transfer of the collided ions. Collisions of hollow fullerenes (C_{60}^+ , C_{70}^+ and C_{78}^+) and a metallofullerene ($Ca@C_{84}^+$) with the fluorinated SAM film showed a series of even numbered fragments (C_{2n}^+) as a result of sequential C_2 -loss processes. However, no SID of C_{60}^+ was observed against the alkanethiolate SAM film. This can be explained by the difference of the effective mass of the fluorinated and the alkanethiolate surfaces.

ACKNOWLEDGMENTS

We thank Professor K. Hiraoka (Yamanashi University) for valuable discussion on the SAM films. We also thank M. Ohno, T. Nakane and T. Iwano (Nagoya University) for supplying the metallofullerene and the higher fullerene samples. The AFM collaboration with T. Takeshita and Professor T. Imae (Nagoya University) is gratefully acknowledged. H.S. thanks the Japanese Ministry of Education, Science and Culture Grants-in-Aid for Scientific Research (B)(2)(No. 09440198) and Scientific Research (B)(2)(No. 10554030) for the support of the present study. The present study was also supported by a Future Program "Advanced Processes for New Carbon Materials" of JSPS.

¹R. D. Beck, P. St. John, M. M. Alvarez, F. Diederich, and R. L. Whetten, *J. Phys. Chem.* **95**, 8409 (1991).

²H.-G. Busmann, Th. Lill, B. Reif, and I. V. Hertel, *Surf. Sci.* **272**, 146 (1992).

³R. D. Beck, J. Rockenberger, P. Weis, and M. M. Kappes, *J. Chem. Phys.* **104**, 3638 (1996).

⁴R. C. Mowrey, D. W. Brenner, B. I. Dunlap, J. W. Mintmire, and C. T. White, *J. Phys. Chem.* **95**, 7138 (1991).

⁵M. R. Morris, D. E. Riedere, Jr., B. E. Winger, R. G. Cooks, T. Ast, and C. E. D. Chidsey, *Int. J. Mass Spectrom. Ion Processes* **122**, 181 (1992).

⁶A. Somogyi, T. E. Kane, J.-M. Ding, and V. H. Wysocki, *J. Am. Chem. Soc.* **115**, 527 (1993).

⁷J. H. Callahan, A. Somogyi, and V. H. Wysocki, *Rapid Commun. Mass Spectrom.* **7**, 693 (1993).

⁸T. Kimura, T. Sugai, and H. Shinohara, *Chem. Phys. Lett.* (in press).

⁹E. R. Williams, G. C. Jones, Jr., L. Fang, R. N. Zare, B. J. Garrison, and D. W. Brenner, *J. Am. Chem. Soc.* **114**, 3207 (1992).

¹⁰G. G. Urquhart, J. W. Gates, Jr., and R. Connor, *Organic Syntheses* (Wiley, New York, 1955), Collect. Vol. III, p. 363.

¹¹G. Liu, P. Fenter, C. E. D. Chidsey, D. F. Ogletree, P. Eisenberger, and M. Salmeron, *J. Chem. Phys.* **101**, 4301 (1994).

¹²H. Shinohara, H. Yamaguchi, N. Hayashi, H. Sato, M. Ohkohchi, Y. Ando, and Y. Saito, *J. Phys. Chem.* **97**, 4259 (1993).

¹³H. Shinohara, M. Inakuma, M. Kishida, S. Yamazaki, T. Hashizume, and T. Sakurai, *J. Phys. Chem.* **99**, 13,769 (1995).

¹⁴H. Shinohara, M. Tanaka, M. Sakata, T. Hashizume, and T. Sakurai, in *Cluster-Assembled Solids*, edited by K. Sattler (Trans Tech, Switzerland, 1996).

¹⁵H. Shinohara, *Adv. Metal Semiconductor Clusters* **4**, 205 (1998).

¹⁶E. Yamamoto, M. Tansho, T. Tomiyama, H. Shinohara, H. Kawahara, and Y. Kobayashi, *J. Am. Chem. Soc.* **118**, 2293 (1996).

¹⁷Z. Xu, T. Nakane, and H. Shinohara, *J. Am. Chem. Soc.* **118**, 11,309 (1996).

¹⁸M. Tanaka, B. Umeda, E. Nishibori, M. Sakata, Y. Saito, M. Ohno, and H. Shinohara, *Nature (London)* **377**, 46 (1995).

¹⁹L. M. Roth, Y. Huang, J. T. Schwedler, C. J. Cassidy, D. Ben-Amotz, B. Kahr, and B. S. Freiser, *J. Am. Chem. Soc.* **113**, 6298 (1991).

²⁰Y. Huang and B. S. Freiser, *J. Am. Chem. Soc.* **113**, 9418 (1991).

²¹C. Yeretizian, K. Hansen, M. M. Alvarez, K. S. Min, E. G. Gillan, K. Holczer, R. B. Kaner, and R. L. Whetten, *Chem. Phys. Lett.* **196**, 337 (1992).

²²Th. Lill, H.-G. Busmann, F. Lacher, and I. V. Hertel, *Chem. Phys.* **193**, 199 (1995).

²³T. Moriwaki, H. Shiromaru, and Y. Achiba, *Z. Phys. D* **37**, 169 (1996).

²⁴F. Aumayr, G. Betz, T. D. Märk, P. Scheier, and H. P. Winter, *Int. J. Mass Spectrom. Ion Processes* **122**, 181 (1992).

²⁵R. D. Beck, P. Weis, J. Rockenberger, R. Michel, D. Fuchs, M. Benz, and M. M. Kappes, *Surf. Rev. Lett.* **3**, 881 (1996).

²⁶T. Tsukuda, H. Yasumatsu, T. Sugai, A. Terasaki, T. Nagata, and T. Kondow, *J. Phys. Chem.* **99**, 6367 (1995).

²⁷R. L. Whetten and C. Yeretizian, *Int. J. Mod. Phys. B* **6**, 3801 (1993).

²⁸J. A. Burroughs, S. B. Wainhaus, and L. Hanley, *J. Phys. Chem.* **98**, 10,913 (1994).